Acta Geologica Polonica, Vol. 62 (2012), No. 1, pp. 129–141

Digital Concentration-Distribution Models – tools for a describing heterogeneity of the hybridized magmatic mass as reflected in elemental concentration of growing crystal

MICHAŁ ŚMIGIELSKI[1], EWA SŁABY[2, 3] AND ANDRZEJ DOMONIK[4]

[1]*Institute of Geology, University of Warsaw, Żwirki i Wigury 93, 02-089 Warsaw, Poland. E-mail: m.smigielski@uw.edu.pl*
[2]*Institute of Geological Sciences, Research Centre in Warsaw, Polish Academy of Sciences, Twarda 51/55, 00-818 Warsaw, Poland. E-mail: e.slaby@twarda.pan.pl*
[3]*Institute of Geochemistry, Mineralogy and Petrology, University of Warsaw, Żwirki i Wigury 93, 02-089 Warsaw, Poland. E-mail: ewslaby@uw.edu.pl*
[4]*Institute of Hydrogeology and Engineering Geology, University of Warsaw, Żwirki i Wigury 93, 02-089 Warsaw, Poland. E-mail: adomonik@uw.edu.pl*

ABSTRACT:

Śmigielski, M., Słaby, E. and Domonik, A. 2012. Digital Concentration-Distribution Models – tools for a describing heterogeneity of the hybridized magmatic mass as reflected in elemental concentration of growing crystal. *Acta Geologica Polonica*, **62** (1), 129–141. Warszawa.

Raster digital models (digital concentration-distribution models – DC-DMs) as interpolations of geochemical data are proposed as a new tool to depict the crystal growth mechanism in a magmatic environment. The Natural Neighbour method is proposed for interpolation of Electron Microprobe Analysis (EMPA) data; the Natural Neighbour method and Kriging method are proposed for interpolating data collected by the LA-ICP-MS method. The crystal growth texture was analysed with the application of DC-DM derivatives: 3D surface models, shaded relief images, aspect and slope maps. The magmatic mass properties were depicted with the application of solid models. Correlation between the distributions of two elements on a single crystal transect was made by operations on the obtained raster DC-DMs. The methodology presented is a universal one but it seems to be significant for the depiction of magma mixing processes and the heterogeneity of the magmatic mass.

Key words: Magma mixing; Crystal growth; Raster digital model; DC-DM, EMPA, LA-ICP-MS.

INTRODUCTION

Melt differentiation is a complex phenomenon, including a multitude of processes related to changes in its composition and its emplacement. These processes are frequently mirrored in heterogeneous growth texture and composition of minerals. More recently, there has been a dynamic increase in research on the nature of crystal heterogeneity observed. A significant part of this research involves investigations of crystal zonation with the use of geochemical methods, including isotope-based methods (e.g. Gagnevin *et al.* 2005a, b; Ginibre *et al.* 2002; Ginibre *et al*. 2004; Ginibre *et al.* 2007; Słaby *et al.* 2007a; Słaby and Götze 2004; Słaby *et al.* 2008). The basic tool commonly applied is identification of the distribution of an element along a linear traverse.

Another tool is electron probe mapping (EMPA) of the distribution of the concentration of an element. However, this method is of lower sensitivity and is usable only for an approximate assessment of crystal composition heterogeneity. The depiction of the crystal geochemical data obtained from measurements along a traverse consists of a Cartesian diagram that includes two variables: location of the measurement points along the traverse and the corresponding element concentration (Gagnevin *et al*. 2005a; Ginibre *et al*. 2002; Ginibre *et al*. 2004; Słaby *et al*. 2007a; Słaby *et al*. 2007b). This methodology exhibits, only to a certain extent, the complexity of crystallisation process in a heterogeneous magmatic mass created by contamination, magma mixing and crystallization. Therefore an attempt has been made to apply multi-dimensional models (widely used in various areas of geology and other science disciplines) for the depiction of these complex processes.

The aim of this paper is to present the methodology developed for the description of local magmatic mass heterogeneity caused by magma mixing processes. The methodology applies depiction and analysis techniques originally developed for raster digital elevation models (DEM) (see for review Konon and Śmigielski 2006). These techniques have been used to analyse digital concentration distribution models (DC-DM) – grid models that present the spatial distribution of element content on a crystal cross-section. Moreover, three different measurement paths of element concentration are discussed in order to assess their usability in creating such models.

METHODS OF DATA COLLECTION

The source data for the raster DC-DM are geochemical data for an element concentration estimated by commonly applied methods: laser ablation ICP-MS and electron microprobe (EMPA) for a single phase.

For the present paper data were collected from alkali feldspars from the Hercynian Karkonosze pluton (Bohemian Massif) and the Archaean Closepet massif (Dharwar craton, India). The samples most suitable for such analytical treatment are those collected in an environment of dynamic crystallization in a heterogeneous magmatic mass. The preferred magmatic bodies are composite plutons and volcanic items originating from magmas derived from compositionally different sources and then extensively stirred. Both the above-mentioned plutons have originated in this way.

Crystals were traversed along parallel lines located at constant distances between each other. Two paths of measurements of the concentration of an element by means of LA-ICP-MS and one by EMPA were proposed (Text-fig. 1). The crystal was analysed along a transect by moving the laser spot at a constant speed of about 10 to 20 μm/s, 10 Hz repetition rate and 80–90 μm laser spot diameter over a thin section (method 1 – LA-ICP-MS continuous traverse) or by different time resolved analysis with 100 repeats within one spot (dwell time 20 ms for all isotopes, 0.943 s/sweep) (method 2 – LA-ICP-MS spot-by-spot) (Text-fig. 1a, b). The 80–90 μm laser spot size was chosen in order to achieve 0.5 mm depth of analysis in method 2.

Concentration was estimated for several dozen elements, including K, Ba, Sr and Rb. The first method resulted in obtaining data on the crystal intersect along parallel profiles spaced ~1 mm from each other. The along-profile measurement resolution was up to 1 measurement per 10 μm. The second method produced an image of in-depth distribution for the same elements. The 20 to 30 LA-ICP-MS spots were aligned at constant ~0.5 mm intervals. The depth of the crater was up to 0.5 mm (1 measurement ablated about 5 μm of the sample). Using EMPA, the crystal was profiled by microprobe point analyses at constant 300 μm intervals along a number of parallel profiles located at 1 mm from each other (method 3 – EMPA) (Text-fig. 1c). All these pro-

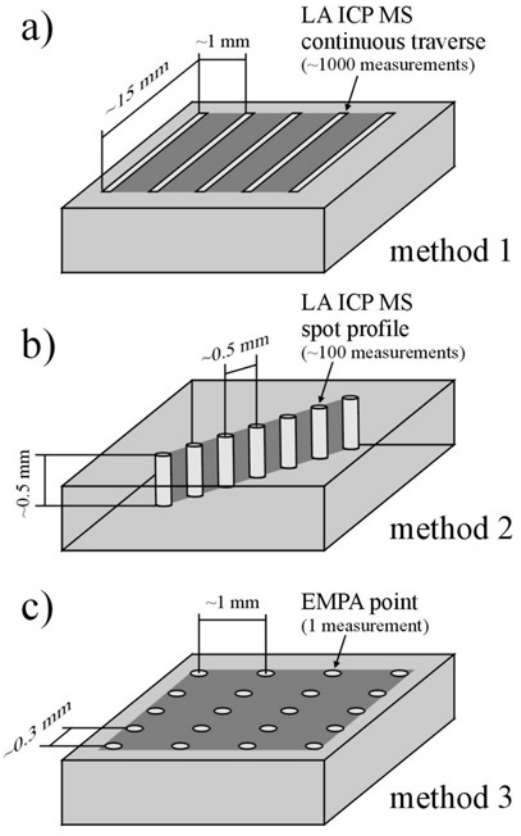

Text-fig. 1. Three methods of geochemical data collection. Dark-grey rectangle shows area of DC-DM interpolation. For more explanations see text

cedures and resolutions are comparable in terms of the financial cost of analysis of a single crystal transect.

Differences in the data collection methods and differences in the element distribution characteristics determined in the preliminary analysis were the reasons for application of slightly different methods for the data processing and their further depiction. These details are indicated in the paper. The developed and presented solutions allowed comparison of the applicability of geochemical data collection methods for creating DC-DM and additional statistical analyses.

DATA PRE-SELECTION

Pre-selection is the first stage of the processing of the source data in order to create a DC-DM for a single crystal. Data pre-selection is a procedure which involves removing selected measurements that could be artifacts or which demonstrate abnormally high or low values that can be explained by the appearance of different phases, e.g. inclusions in the crystal.

The dataset obtained by methods 1 and 2 (LA-ICP-MS), due to the high measurement resolution along the profile, allowed precise calculation of the local gradient. This gradient was determined as the ratio between adjacent concentration measurements (higher value divided by lower value). On the base of this calculation data featuring a quotient >2 were removed (Text-fig. 2). An abnormally high gradient was usually found for the first few or last few laser impulses using sampling method 2. The most probable reason for a high gradient at the surface is splitting off of small fragments of a mineral. On the other hand, measurements recorded for the last pulses bear errors due to the uneven floor of the crater (the deeper the crater, the more uneven the floor becomes), and mixing of the material evaporated from the floor and the walls of the crater.

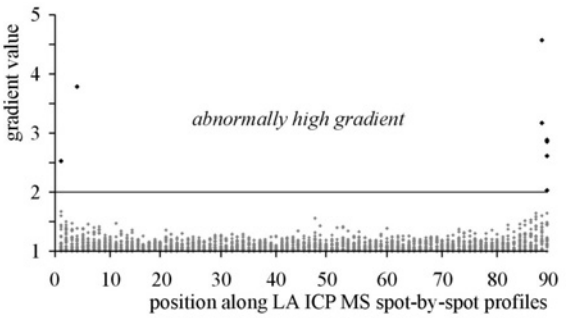

Text-fig. 2. Ba concentration gradient in the alkali feldspar tested by LA-ICP-MS-spot-by-spot-method 2. Horizontal axis: consecutive sampling by laser ablation along 25 vertical profiles. Vertical axis: value ratios for adjacent measurements

In order to obtain a genetically homogeneous dataset, showing only the composition of a single phase under test, fragments featuring abnormally low or high values of the analysed element concentrations that indicate inclusions should also be omitted. In alkali feldspars which originated from magma mixing processes, this concerns mainly inclusions of plagioclases located inside the crystal. Inclusions of plagioclases were removed on the basis of major element concentration in the investigated phase, e.g. potassium being the major element for K-feldspar (Text-fig. 3). Some anomalous high values of Ba, Sr and Rb measured inwards the profiles of more than 10 times the average were also deleted. Taking into consideration end-member magma composition (mafic and felsic components) in term of Ba, Sr and Rb and information on the degree

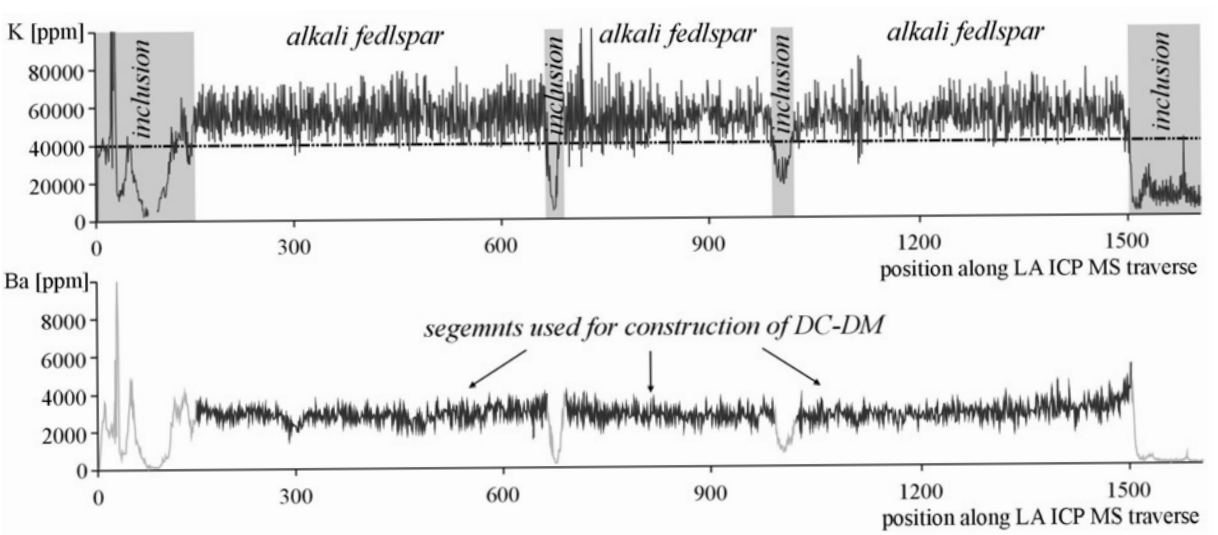

Text-fig. 3. Potassium and barium concentration along a single LA-ICP-MS-traverse-method 1 (Closepet feldspar). Dotted-dashed line: K = 40000 ppm – approx. lowest potassium concentration in alkali feldspar. For further explanation see text

of magma mixing and theoretical K-feldspar composition (Slaby *et al.* 2008), these high values can be attributed to small inclusions of accessory minerals. Only as little as 1 to 3% of the input data was eliminated for a single analysed sample.

Data prepared in the way described can be used as a source data for the interpolation of a DC-DM. However, the removal of inclusions from profiles can be the reason for significant gaps, where from several up to even dozens of measurements are missing (Text-fig. 3). At the next stage of data processing, those vacant areas were filled with interpolated values. Therefore, the obtained models show a presumed element distribution for K-feldspar without inclusions.

Statistical analysis of the collected data should be made after pre-selection but prior to interpolation. Still, gaps created by pre-selection in profiles can influence parameters calculated and based on adjoining measurements, such as on the value of the Hurst exponent. The Hurst exponent, originating from nonlinear dynamics and based on the fractal properties of Brownian motion, seems to be the most appropriate factor for the quantitative description of crystal geochemical heterogeneity. A complete description of the application of methods for the fractal analysis of geochemical data, as well as a discussion of the interpretations of the results of the analyses, was provided by Domonik *et al*. (2010). This paper is restricted to the description of the pre-selection method for data to be used further for fractal analysis, and to techniques applied for interpolation as well as for depiction of the results of interpolation.

The Hurst exponent is frequently used for the detection of trends and the 'memory effect' in chaotic processes, also in magma crystallizing processes (Hoskin 2000). Quantitative analyses of variable data series, based on determination of the Hurst exponent are successfully applied in various fields of science: natural, economic, and medical (Yang and Lo 1997; Peters 1997; West 1990). The Hurst exponent is sensitive to those subtleties of the stochastic process under analysis that are not detected by classic statistical methods.

Several methods are applied for assessment of the value of the Hurst exponent (*H*), such as the dispersion method, spectral method and autocorrelation estimators. *R/S* analysis, which was introduced by Hurst (1951), and is the outcome of his discriminating research over a long period into the 'memory effect', is ranked among the most popular methods. In this paper the *R/S* analysis method was applied. *R/S* analysis is commonly known as the Rescaled Range Method.

Summarizing the problems presented above, we propose herein five methods of data pre-selection. We propose to make and compare statistical analyses: a) for raw data with mineral inclusions not removed; b) for an integrated profile (joining all traverse sectors to one single item) after inclusion deletion based on the major element content in the phase examined; c) for an integrated profile as one item after inclusion deletion based on the content of a selected trace element in the phase examined ; d) for particular traverse sections between deleted inclusions (based on the major element content); e) for an integrated profile after inclusion deletion (on the basis of major element content in the main phase examined), and afterwards divided into sectors based on the content of a selected trace element. Comparison of differences between these approaches is necessary to recognise the influence of data pre-selection on statistical analysis.

GEOCHEMICAL DATA INTERPOLATION

In order to develop DC-DMs for selected elements, we have applied the Kriging interpolation method and the Natural Neighbour interpolation method. DC-DMs consist of grid nodes with X and Y parameters determining the node location on the transect surface through the crystal against a local reference system. The third parameter for each node is Z, determining the element content in concentration units (e.g. ppm).

In the case of source data collection with the application of laser ablation measurements by moving the laser spot at a constant speed along the transect (method 1), the Kriging interpolation method was preferred (Cressie 1990). The Kriging method is based on variograms allowing the introduction of empirical parameters such as length scale, data repeatability and anisotropy into the interpolation procedure. These parameters provide characteristics of processes conditioning the measurement values, thus enabling the optimising of the Kriging method calculations and improvement of the quality of the interpolation (Cressie 1990; Chiles and Delfiner 1999). Due to the large difference between the number of measurements collected along a profile (from 800 up to 1600) and the number of profiles (up to a dozen), the obtained distribution models average the element content along the profile. As a consequence, the models show major trends for elemental variations with regard to the collected source data. The resolution of the models was from 50 up to 250 micrometres depending on the profile spacing and the number of profiles.

The Natural Neighbour interpolation method was applied to data collected by means of EMPA (method 3) and LA-ICP-MS (method 2). This method applies the idea of Voronoi cells (Voronoi 1907) to assign weights to real measurements, this being the basis for averaging

node values in the interpolated grid (Sibson 1981). In cases where the data featured a distinct zonation (as in most of the feldspars tested from Karkonosze massif), data distribution directional anisotropy was used. For data obtained with application of LA-ICP-MS (method 2), the in-depth resolution was ~5 micrometres, and the horizontal resolution was from 50 to 200 micrometres. Because of this difference between in-depth and cross-wise resolution depictions of the model were exaggerated up to five times. This fact should be considered in the subsequent interpretation. For models obtained with application of the EMPA method, the resolution was from approx. 150 to 300 micrometres depending on the spacing between determinations (point analyses).

DEPICTION METHODS AND QUALITATIVE SURFACE ANALYSIS

The next step is depiction of interpolated surface models and their qualitative analysis. The qualitative analysis of a DC-DM is based on its shape and calculated derivatives and is similar to the analysis of digital terrain elevation models (DTEMs) (e.g. Konon and Śmigielski 2006). Several different depiction options were tested. DC-DMs were visualised with the application of classic isoline maps (Text-fig. 4a), 3D surface models (Fig. 4b, 6a), shaded relief images / reflectance maps (Yoeli 1965) (Text-fig. 5), aspect maps and slope maps (Text-fig. 6b, c).

3D surface depiction was preceded by a resolution multiplication procedure without model recalculation (spline smoothing). This procedure implies the insertion of empty lines or columns between the interpolated grid lines or columns respectively. The next step is filling these with interpolated data obtained by application of a spline-type function based on polynomial functions (e.g. Green and Silverman 1994). This procedure has no significant influence either on the data distribution or on the data value but enables obtaining images of a higher resolution, thus improving the graphic value of the depiction and facilitating the qualitative analysis thereof (Text-fig. 4, 5, 6). The location of the measurement

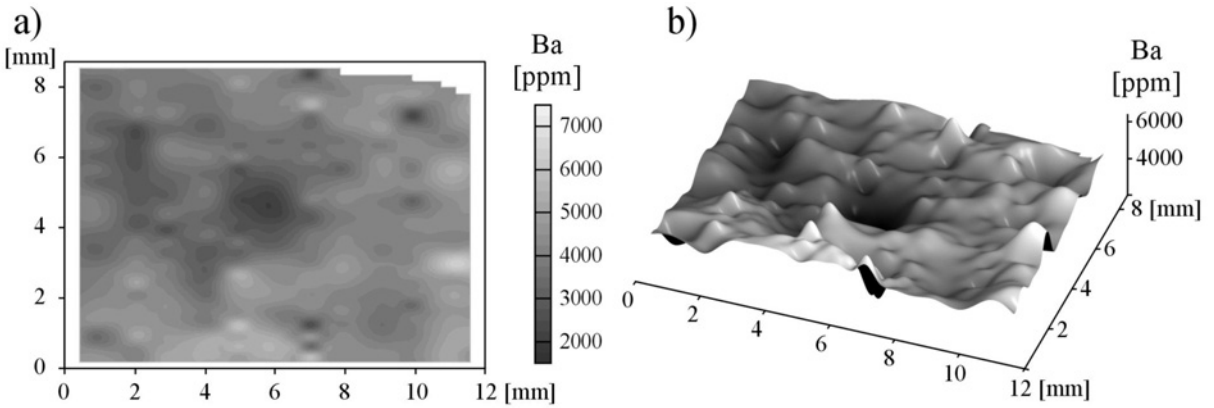

Text-fig. 4. Example of DC-DM of barium in Closepet feldspar. Data collected with EMPA – method 3: a – isoline map; b – 3D surface model

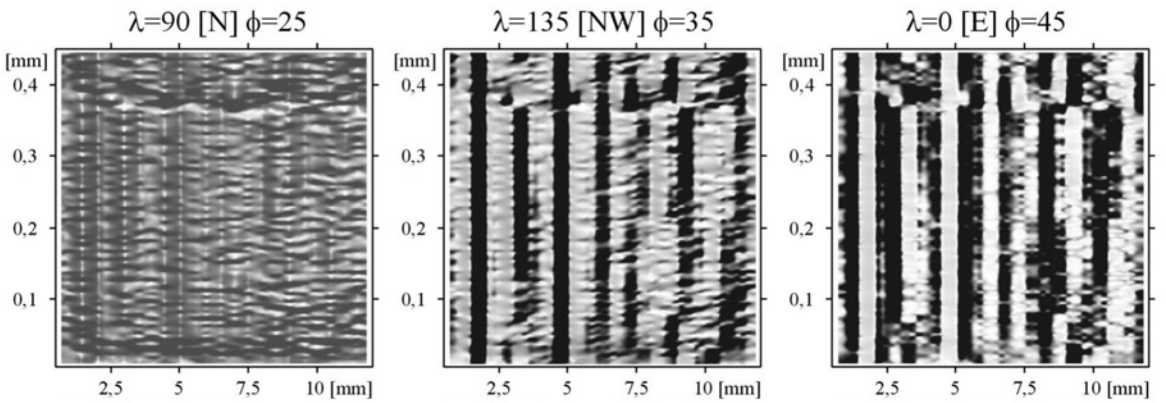

Text-fig. 5. Reflectance maps of the DC-DM for Sr in feldspar from Karkonosze pluton. Light position angles: λ – horizontal, ϕ – vertical (based on data collected by LA-ICP-MS method 2). Note that zonation clearly visible when illuminated from perpendicular (λ=0) or oblique (λ=135) direction and almost invisible when illuminated from parallel direction (λ=90). Parallel illumination reveals minor changes of concentration along zones

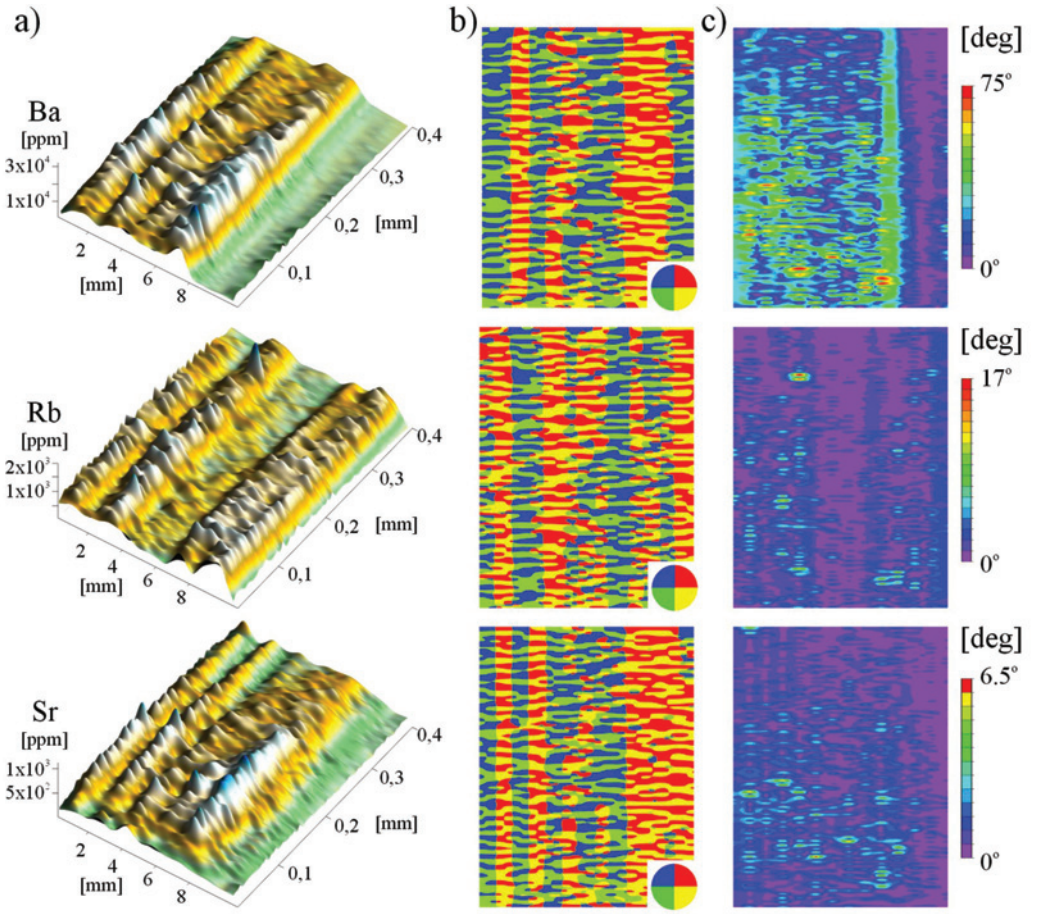

Text-fig. 6. Example of DC-DM of barium, strontium and rubidium from the same crystal intersect (Karkonosze feldspar); a – 3D surface model; b – maximum gradient direction map simplified to 4 sectors (circle shows maximum gradient direction – direction of value decrease); c – maximum gradient value (same exaggeration for all three elements)

point was given in micrometres against the local reference system, the element content in ppm. Thus, the obtained 3D surfaces do not make any geometrical sense and their vertical scale may be adjusted arbitrarily in order to obtain the best image possible for the 3D data interpretation.

In order to visualise and analyse various morphology aspects of DC-DMs, shaded relief images (reflectance maps) with several different lighting directions were used (Cooper 2003) (Text-fig. 5). Reflectance maps were based on the Fleming-Hoffer algorithm (Fleming and Hoffer 1979) which is used for the determination of maximum gradient values and maximum gradient directions for each grid node of an analysed surface, based on four adjacent nodes. The Fleming-Hoffer algorithm ensures a high degree of accordance between the shape of the surface and the calculated parameters (Jones 1998; Zhou and Liu 2004). Reflectance was calculated based on the maximum gradient values and directions with application of the Lambertian reflection model (Pelton 1987), with lighting direction azimuth (λ) and light ray angle (ϕ) as the parameters (Text-fig. 4).

Isoline maps, 3D surface models and shaded relief images thus prepared may be used for an initial assessment of the distribution character for selected elements. This assessment includes determination of areas of high and low element concentration as well as preliminary determination of zoning or other types of growth texture. Estimation of the growth texture is of particular importance. It provides information on the character of the process controlling crystal formation or its further overgrowth.

The following parameters were used in further qualitative analysis: direction of maximum gradient of the element concentration (aspect map) and maximum value of local gradient (slope map) (Text-fig. 6b, c). These parameters were obtained at the shaded relief images generation stage with application of the Fleming-Hoffer algorithm (Fleming and Hoffer, 1979), as described above. Aspect maps present directions of maximum decrease in element concentration (0-360°) over the in-

terpolated surface. For simplification these azimuths can be averaged into 4 or 6 sectors (Text-fig. 6b). Slope maps present the rate of change of element concentration as an angle of slope in the direction of its maximum decrease (0–90°). As the vertical scale of the models can be adjusted arbitrarily, the value of the exaggeration should be chosen to provide a wide range of angles (Text-fig. 6c). Too small an exaggeration will produce flat models with slope angles varying only between 0 and 1°, while too large an exaggeration will create models with all slope angles close to 90°. In order to facilitate comparison between gradient of concentration for different elements on the same cross-section, the same exaggeration should be used whenever possible (Text-fig. 6c).

Aspect and slope maps were used for further determination of the element distribution pattern within a crystal. They show directions of the propagation of those patterns (aspect map) and the dynamics in changes of element concentrations (slope map). Thanks to the simplification provided by slope and aspect maps they can be used for a preliminary determination of the relationship that occurs between various elements and their behaviour during crystallization (Text-fig. 6).

SEMI-SOLID AND SOLID MODELS

Raster images (EMPA element distribution mapping) combined with in-depth profiles obtained by LA–ICP-MS data processing (DC-DMs, method 2) enable mutual verification of both geochemical data acquisition methods and the obtaining of a better three-dimensional insight into the growth texture (Text-fig. 7). This technique is of particular importance when the depiction of the spatial distribution of an element and the analysis of such a distribution in perpendicular cross-sections are required. In the case of EMPA mapping such an analysis is possible if the element concentration is heterogeneous. For the collected data, this option was possible for Ba only. For the other trace elements analysed (Rb, Sr), the EMPA detection limit and narrow concentration range are factors that preclude mapping. The proposed technique is a significantly cheaper alternative to raster (voxel) solid models that completely show the three-dimensional distribution of elements within a crystal. Theoretically, such a distribution can be obtained by interpolation of data collected from a number of parallel LA-ICP-MS in-depth profiles made for a number of intersects.

Interpolation and depiction techniques for solid models can also be used for creating conceptual models of the heterogeneity of the magmatic mass in which the crystal is migrating and growing. To obtain this, DC-DMs of the same element should be developed for a number of specimens from different (with regard to any parameter) parts of a single crystalline massif. Then, the obtained DC-DMs should be combined as a solid model. Such a conceptual model can provide more detailed insight into the composition of the magmatic mass than data provided by whole rock composition. Whole rock composition provides average information about the degree of magma hybridization but cannot show the detailed pattern of heterogeneity of the local domains within the whole magmatic mass. Combining both single crystal analyses and whole rock analyses, we

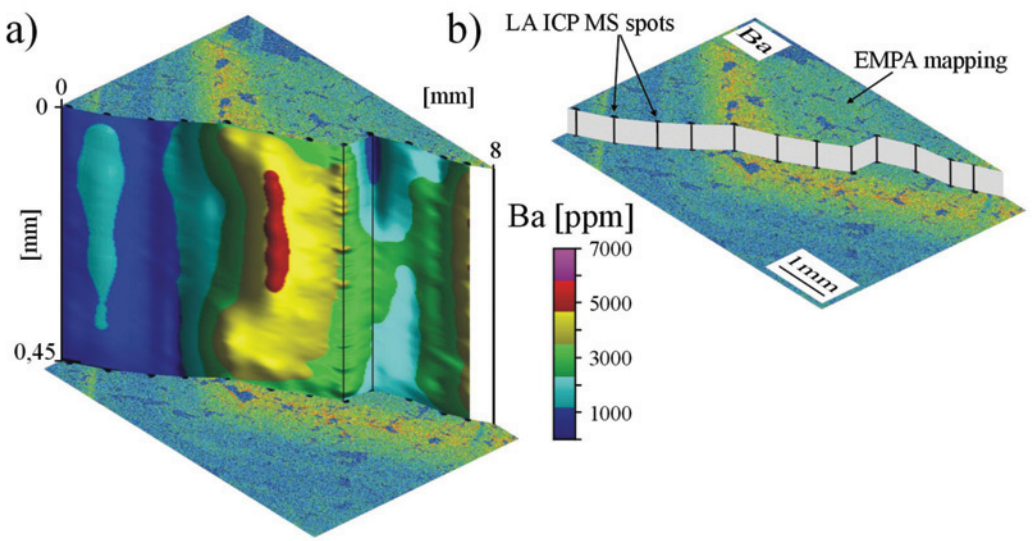

Text-fig. 7. Ba distribution model done for crystal intersect (based on data collected by LA-ICP-MS-method 2), compared with crystal surface scanning image (microprobe method). In order to show two surfaces the EMPA mapping was cut, its part thereof was moved downwards: a – exaggerated; b – scheme showing true proportions

can gain an idea to what extent the pattern of magma domains, reconstructed on the basis of crystal geochemistry, reflects the degree of magma blending gained from bulk rock composition. Thus, the objective of such a model is to present changes in element concentration in an analysed crystal with regard to a chosen parameter (e.g. whole rock chemistry, degree of hybridisation, position of specimen in the massif. etc.). Also, this can be useful for statistical and quantitative analysis of the relationship between the geochemical pattern and the chosen parameter.

A model for the Karkonosze massif, developed by combining numerous DC-DMs from intersects of feldspars originated from crystallization within a heterogeneous magmatic mass featuring different degrees of hybridisation, could be regarded as an example of the type of model discussed above (Text-fig. 8). The degree of hybridisation was calculated based on the Fourcade-Allegre algorithm (Fourcade and Allegre 1981), using whole rock analyses. The end-members of the magma composition were taken from the Słaby and Martin model (2008). The solid model was developed based on a data set featuring: X, Y – measurement location coordinates on the DC-DM from a single feldspar; Z – element content of DC-DM at X, Y location [ppm]; P – degree of hybridisation of the magma from which the feldspar crystallised. The X, Y and P are assigned to respective directions according to the three-dimensional reference system, which resulted in obtaining a full solid model by interpolation based on the Z value (Text-fig. 8a). The solid model interpolation was made with the application of the Kriging method in its three-dimensional version. The model developed is an conceptual presentation of the heterogeneity of the open system in which the feldspar crystallisation occurred. The aim of this particular model is to give insight into a complicated pattern of magma mixing, i.e., a pattern of a magmatic mass in which a

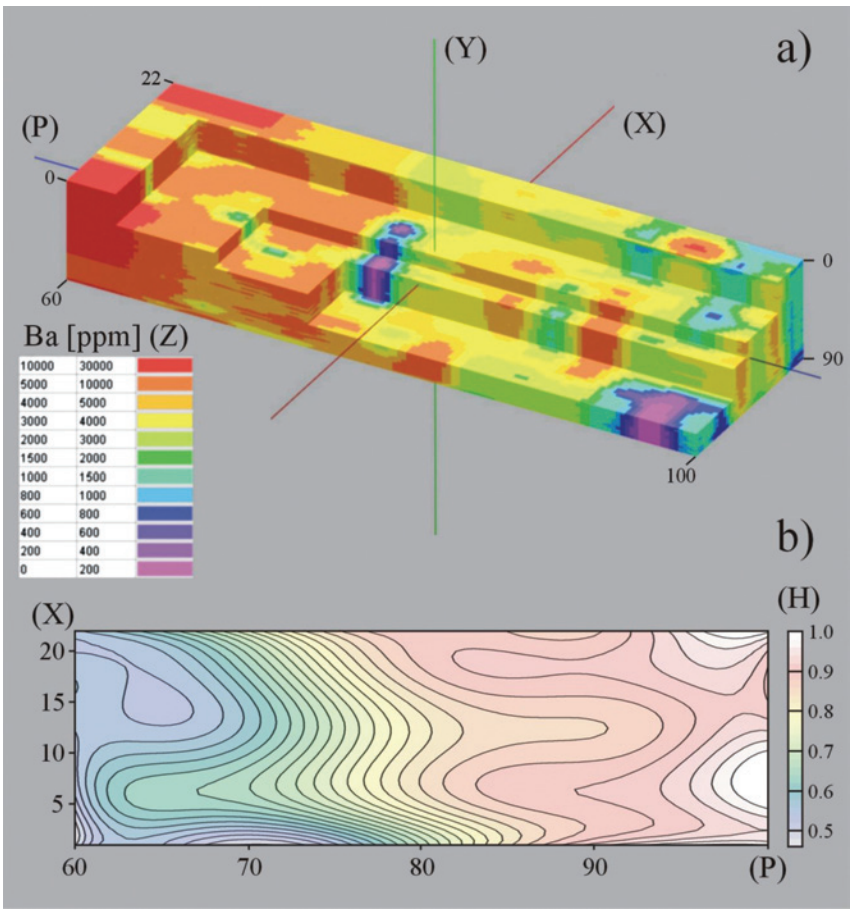

Text-fig. 8. a – Three-dimensional Ba distribution (Z) solid model of conceptual magmatic mass featuring an increasing degree of magma hybridisation (P). The input of mantle-derived magmas with the highest barium concentration decreases from left to right due to the increasing content of crustal magmas with a low Ba concentration. The model shows a complicated image of two environments penetrating each other, with a small number of coherent (end-member magma) domains and a large number of active (mixed) domains; b – Hurst exponent (H) distribution in a conceptual magmatic mass as a polynomial surface map for 6th order trend. Note strong negative correlation between barium concentration and Hurst exponent value. For more explanations see text

migrating crystal has incorporated its components through diffusion and advection. As mentioned above, the model is an abstract and not an actual depiction of the magmatic mass heterogeneity.

Such an abstract solid model can by used for further statistical analysis of the magmatic mass. In the example presented, the Hurst exponent (H) was calculated for every single in-depth LA-ICP-MS profile in the model. Thus, after the fractal analysis and interpolation with the application of polynomial trend analysis (Draper and Smith 1998), the solid model (with four parameters: X, Y, P, Z describing each point) was transformed into a surface model described with three parameters (X, P, H) (Text-fig. 8b).

The model (Text-fig. 8a, b) shows that, even if the magmatic mass moves toward homogenization and the whole rock composition testifies in favour of full magma blending, the data derived from crystal geochemistry still reveal areas of heterogeneous magma. Incorporation of elements into the growing phase demonstrates decreasing dynamics reflected in an increasing Hurst exponent value. Even if the magmatic mass is not fully blended, the behaviour of elements in the mass is persistent in contrast to that in the poorly homogenised magma domains, where the elements tend to behave anti-persistently. The Hurst exponent is a very effective tool in describing changes in crystallization dynamics that proceed from hybridized magmas.

CORRELATION OF ELEMENT DISTRIBUTIONS WITHIN A SINGLE CRYSTAL

Laser ablation enables the simultaneous collection of data on the concentration of many different elements and, consequently, the development of several DC-DMs showing different element distributions within the same intersect. This enables the analysis of the mutual rela-

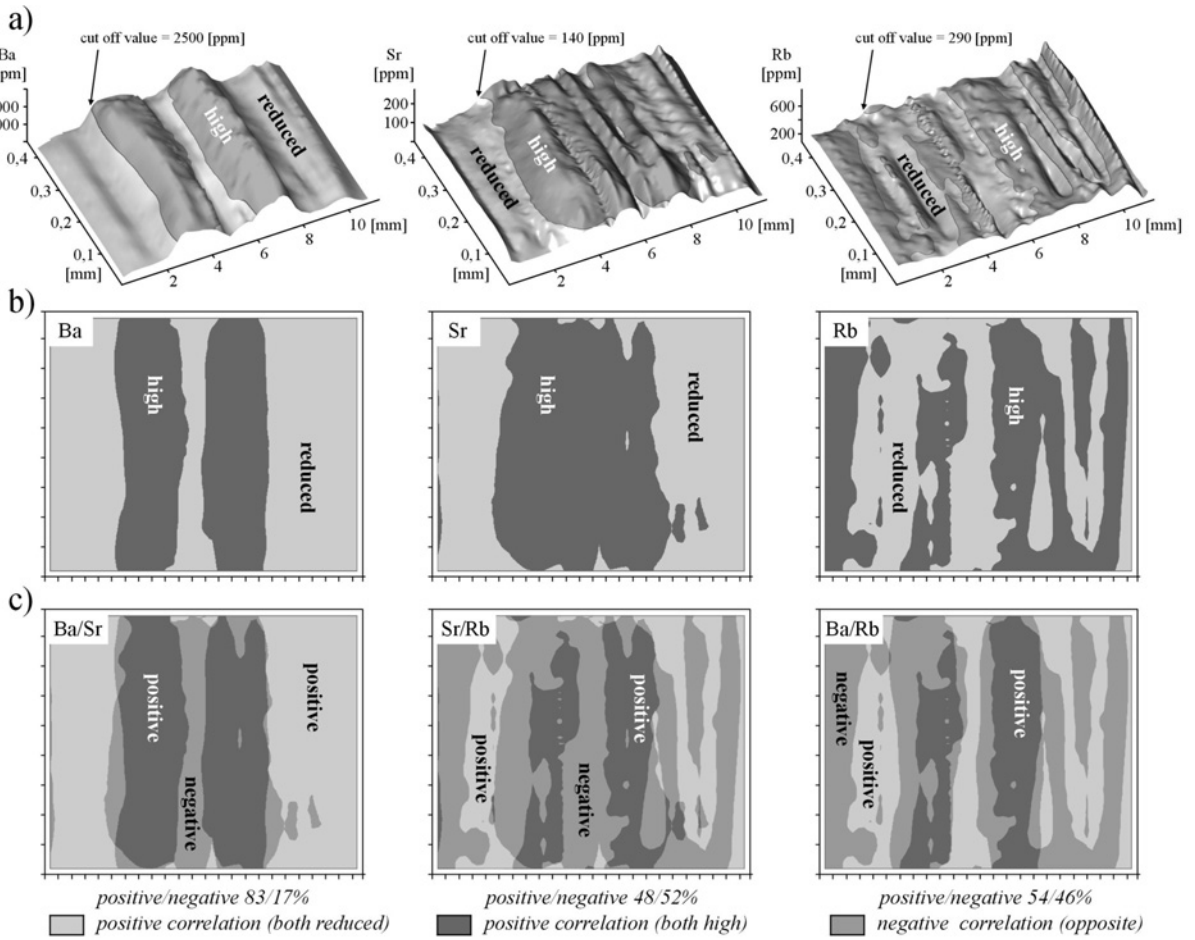

Text-fig. 9. Diagram showing the procedure of correlation of the distribution of elements within a single crystal using relative concentration values: a – 3D surface models of barium, strontium and rubidium with average concentration indicated; b – transformation of element DC-DM into binary (high/reduced) model based on values compared to an average concentration for a single transect; c – output models showing from left to right level of correlation between spatial distribution of Ba and Sr, Ba and Rb, Sr and Rb respectively

tionships between two elements during their incorporation into the crystal. In order to achieve this, we propose to apply two different procedures for comparative, qualitative analysis.

The first procedure consists of comparing the relative concentration values for both elements determined against their average concentration (Text-fig. 9a). This average value may be calculated for each element, based either on all data collected on the analysed intersect, or by averaging the average values for each profile (in case the numbers of measurements in the profiles differ due to deletion of the inclusions). The next step consists of assigning the value of 1 to the areas of the DC-CM above the average, and the value of –1 to the areas below the average for each analysed element separately, with the application of a filtering procedure (Text-fig. 9b). Such prepared DC-DMs were divided one by the other by means of the application of surface calculations. Output values of 1 mean the mutual covering of higher and reduced content areas and values of -1 mean the opposite situation (1/1=1 and -1/-1=1, but 1/-1=-1) (Text-fig. 9c).

The second method consists of discriminating (with application of the first derivative) between those areas of the DC-DM where the concentrations of an element increase or decrease. Such an analysis is made in a direction parallel to the direction of crystal growth in order that the potential growth zonation can be visualised. Filtration should be applied in order to assign a value of 1 to the areas of concentration increase and of -1 to the areas of concentration decrease (Text-fig. 10a). Subsequently the same procedure would be followed for the DC-DM showing the concentration of the second element. Finally, both surfaces would be divided one by the other. In the output model, positive values are assigned to areas where concentrations of the two elements increase or decrease simultaneously. Negative values are assigned to the areas where the concentration of one of the elements increases while that of the other decreases (Text-fig. 10c).

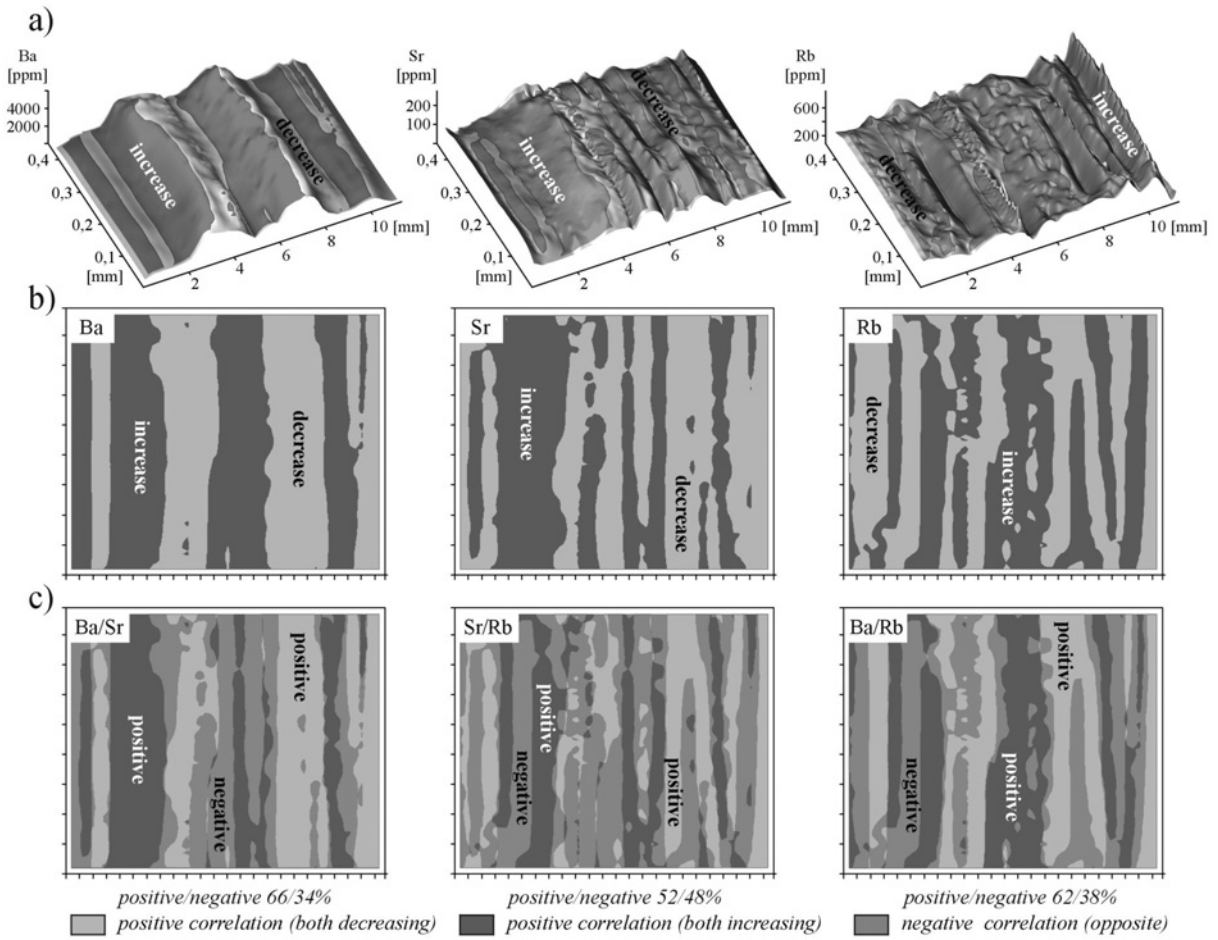

Text-fig. 10. Diagram showing the procedure of correlating the distribution of elements within a single crystal using gradient direction: a) 3D surface models of barium, strontium and rubidium with relative gradient direction indicated; b) transformation of element DC-DM into binary (increase/decrease) model based on gradient direction; c) output models showing from left to right level of correlation between spatial distribution of Ba and Sr, Ba and Rb, Sr and Rb respectively

Both of the described above output models present the level of compatibility between the elements analysed. The first of them shows the compatibility grade of the concentration value of elements while the second shows the compatibility grade between changes in the concentration of elements. These mutual relationships can be quantified and described as the quotient of the number of grid nodes of the output DC-DM featuring positive values (compatibility) and the total grid number. When the values are close to 100% of the covered area, this means that the distribution or concentration change of two elements is fully compatible (positive correlation). A value close to 0% indicates the opposite distribution of elements (negative correlation). In such a situation the distribution of the elements is completely incompatible. Concentration highs of one element coincide with lows of another and increases in concentration coincide with decreases. Values close to 50% are suggestive of the absence of any relationship so far as the analysed model has a microdomain character. In the case where the two elements show a perfectly compatible distribution on half of the analysed transect area, while the other half features an opposite relationship, the result will also be 50%. Thus, the value itself cannot be used for describing relationships between the elements without any regard to the qualitative analysis of spatial distribution using DC-DM products. Please note that, even in the case of a perfectly positive or perfectly negative correlation of two-element distribution, the result will always differ from 100% or from 0%, respectively. This fact is due to cumulative measurement error and to interpolations based on point observations.

A high level of positive correlation between analysed elements (>90%) or a high level of negative correlation (the same as a low positive value of <10%) provides evidence of a preserved original distribution and a lack of secondary processes affecting the relationship between the distributions of the elements. Both of these situations also indicate similar and relatively slow diffusion rates of the elements in the melt. A lack of correlation suggests larger differences in diffusion rates or the influence of redistribution processes that altered and changed the initial correlation. The above-presented methods of analysing the concentrations of elements have been applied to track differences in the diffusion progress during the incorporation of elements into the crystal (Słaby *et al.* 2011).

DISCUSSION

The application of numerous methods of geochemical data collection, depiction techniques and model analysis methods, enabled the comparison of their applicability to the description of the heterogeneity of the distribution of an element within a single crystal. The major advantage of the profiling done by laser ablation across the crystal surface (method 1) is the large number of data acquired along a profile (approx. 100 measurements per 1 mm of profile length). LA-ICP-MS profiling also provides high precision determinations of the element content (1σ error equal to 1–7% of the measured value). Data acquired by laser ablation allow comparative analysis for various elements and facilitate the location of inclusion zones. However, the quality of a DC-DM is limited by the number of parallel profiles made within the crystal. If only a few profiles are made, the large difference between the amounts of data collected in a perpendicular directions hinders the interpolation and is the reason for the model constituting a significant averaging of the input data. Both the precision and reliability of the model increase with the number of profiles. Theoretically, if profiling is made every 100 micrometres (spot diameter approx. 80–90 micrometres), the measurement number can reach 1000 per sq. mm. This value provides nearly continuous information on element content within a mineral, such an image being similar (in terms of coverage) to microprobe scanning. However, the prohibitive costs of LA-ICP-MS would restrict its use in this case. The collected data are suitable for calculating the Hurst exponent and they even enable the determination of its value for selected parts of the profile, thus allowing application of interpolation and depiction methods for the determination of distribution trends in the Hurst exponent (Słaby *et al.* 2012).

The most important advantage of laser ablation in-depth profiling (method 2) is obtaining the element distribution along a cross-section perpendicular to the crystal intersect. It facilitates comparison of surface data with in-depth results, and leads to a more complete recognition of changes in the chemical composition of a mineral. Additional advantages are high sampling resolution (along the profile) and the number of data, enabling calculation of the value of the Hurst exponent. The reliability and resolution of models showing element distribution along a transect depend on the spot spacing. A distance of approx. 250–500μm between adjacent spots is sufficient to obtain a model showing the element distribution microtexture if approx. 20–30 in-depth craters are made along the transect line. Sampling resolution should be adjusted to the level of heterogeneity and, in the case of zoned texture, to the width of zones (Słaby *et al*. 2011). Still, this model has disadvantages: a difference between the vertical resolution and horizontal resolution, and a difference between the in-depth profiling range and the transect line

length. Usually, the transect line is at least 10 times longer than the in-depth range, thus forcing the use of scale exaggeration in depicting a model. Such exaggeration must be taken into account during the analysis and interpretation of the DC-DM.

For data obtained by microprobe point analysis (method 3), the model accuracy depends on the density of measurement points, this being, unfortunately, limited due to the high costs and long time involved in a single analysis. The detection limit, though higher than in the EMPA scanning method, is still a significant impediment as it obviously narrows the database to a few trace elements.

Among all the tested methods for depiction and qualitative analysis of interpolated element distribution models, the 3D shaded relief models appear to be the most suitable for a preliminary determination of the distribution texture for the analysed elements. Models showing the element concentration gradient values and the maximum gradient direction proved to be the best method for describing the dynamics of elemental variation, and for precisely demarcating the borders between zones featuring dramatically different concentrations.

Two methods of displaying the correlation between the distributions of two elements over the same transect were tested: 1) the method based on relative element concentration, and 2) the method based on gradient direction analysis over a transect perpendicular to the crystal growth zones. The first method preferentially exhibits a general correlation grade between elements over the entire crystal transect. This is due to the fact that the average concentration value is used to determine the local relative concentration of an element (Text-fig. 9). The other method is suitable for comparing the correlations at a local scale because compared gradient is calculated for each grid node based on adjacent nodes only (Text-fig. 10).

The procedure in processing the geochemical data consists first in data pre-selection in order to ascertain the homogeneity of the data set to be analysed. The preselection methodology, as presented in this paper, may not be regarded as a universal method. That is due to the fact that data pre-selection depends on the measurement method of the element concentration and on the character of element distribution within the crystal. Nevertheless, inclusion deletion is required, as otherwise the results of both statistical analysis and depiction would be significantly biased. The next step is carry out statistical analysis including (as far as the number of data allows) fractal analysis. At this stage of testing, inclusion deletion prior to statistical analysis is important. Further steps include: interpolation, preliminary depiction of the spatial distribution of an element within the crystal and analysis of derivatives from the models. The analysis can be made more thorough by correlating distributions of various elements on a single transect and constructing models showing microtextures on perpendicular planes.

CONCLUSIONS

The proposed new methodological approach encompasses processing of geochemical data and further depiction of the processed data, which provides a strong basis for the genetic interpretation of the phases crystallized in a magmatic environment. The discussed methodology is undoubtedly particularly suitable for non-homogeneous environments featuring high compositional variability and chaotic domain distributions, with either an increase or dramatic decrease in component concentration and temperatures. Such an environment is formed by interacting magmas of contrasting composition. Similar environments may also be created by post-magmatic fluids, whose influence on magmatic phases can lead to a selective component exchange within a crystal. The secondary phase non-homogeneity resulting from such a reaction with fluids and/or vapour can be tested using the methods described above.

REFERENCES

Chiles, J.P. and Delfiner, P. 1999. Geostatistics: Modeling spatial uncertainty, 350 p. Wiley & Sons; New York.

Cooper, G.R.J. 2003. Feature detection using sun shading. *Computers & Geosciences*, **29**, 941–948.

Cressie, N.A.C. 1990. The origins of Kriging. *Mathematical Geology,* **22**, 239–252.

Draper, N.R. and Smith, H. 1998. Applied regression analysis. Third Edition. John Wiley & Sons, Inc.; New York.

Domonik, A., Słaby, E. and Śmigielski, M. 2010. The Hurst Exponent as The Tool for Description of Magma Field Heterogeneity Reflected in The Geochemistry of Growing Crystals. *Acta Geologica Polonica*, **60**, 437–443.

Fleming, M. D. and Hoffer, R. M. 1979. Machine processing of Landsat MSS data and LARS Technical Report 062879. Laboratory for Applications of Remote Sensing, Purdue University; West Lafayette, USA.

Fourcade, S. and Allegre, C.J. 1981. Trace element behavior in granite genesis: a case study. The calc-alkaline plutonic association from Querigut complex (Pyrenees, France). *Contributions to Mineralogy and Petrology,* **76**, 177–195.

Gagnevin, D., Daly, J.S., Poli, G. and Morgan, D. 2005a. Microchemical and Sr isotopic investigation of zoned K-

feldspar megacrysts: insights into the petrogenesis of a granitic system and disequilibrium crystal growth. *Journal of Petrology,* **46**, 1689–1724.

Gagnevin, D., Daly, J.S., Waight, T., Morgan, D. and Poli, G. 2005b. Pb isotopic zoning of K-feldspar megacrysts determined by laser ablation multiple-collector ICP-MS: insights into granite petrogenesis. *Geochimica and Cosmochimica Acta,* **69**, 1899–1915.

Ginibre, C., Wörner, G. and Kronz, A. 2002. Minor- and trace-element zoning in plagioclase: implications for magma chamber processes at Parinacota volcano, northern Chile. *Contribution to Mineralogy and Petrology*, **143**, 300–315.

Ginibre, C., Wörner, G. and Kronz, A. 2004. Structure and Dynamics of the Laacher See magma chamber (Eifel, Germany) from major and trace element zoning in sanidine: a cathodoluminescence and electron microprobe study. *Journal of Petrology,* **45**, 2197–2223.

Ginibre, C., Wörner, G. and Kronz, A. 2007. Crystal zoning as an archive for magma evolution. *Elements,* **3**, 261–266.

Green, P.J. and Silverman, B. W. 1994. Nonparametric Regression and Generalized Linear Models. Chapman and Hall; London.

Hoskin, P.W.O. 2000. Patterns of chaos: Fractal statistics and the oscillatory chemistry of zircon. *Geochimica et Cosmochimica Acta*, **64**, 1905–23.

Hurst, H.E. 1951. Long-term storage capacity of reservoirs. *Transactions of the American Society of Civil Engineers*, **116**, 770–808.

Jones, K.H. 1998. A Comparison of algorithms used to compute hill slope as a property of the DEM. *Computers & Geosciences*, **24**, 315–323.

Konon, A. and Śmigielski, M. 2006. DEM-based structural mapping; examples from the Holy Cross Mountains and the Outer Carpathians, Poland. *Acta Geologica Polonica,* **56**, 1–16.

Pelton, C. 1987. A computer program for hill-shading digital topographic data sets. C*omputers & Geosciences*, **13**, 545–548.

Peters, E.E. 1997. Teoria chaosu a rynki kapitałowe. Nowe spojrzenie na cykle, ceny i ryzyko. WIG-Press; Warszawa.

Sibson, R. 1981. A Brief Description of Natural Neighbour Interpolation. In: V. Barnett (Ed.), Interpreting Multivariate Data. John Wiley and Sons, New York, p. 21–36.

Słaby, E. and Götze, J. 2004. Feldspar crystallization under magma-mixing conditions shown by cathodoluminescence and geochemical modelling – a case study from the Karkonosze pluton (SW Poland). *Mineralogical Magazine*,**64**, 541–557.

Słaby, E., Galbarczyk-Gąsiorowska, L., Seltmann, R. and Műller, A. 2007a. Alkali feldspar megacryst growth: geochemical modelling. *Mineralogy and Petrology,* **68**, 1–29.

Słaby, E., Götze, J., Wörner, G., Simon, K., Wrzalik, R., Śmigielski, M. 2008. K-feldspar phenocrysts in microgranular magmatic enclaves: A cathodoluminescence and geochemical study of crystal growth as a marker of magma mingling dynamics. *Lithos,* **105**, 85–97.

Słaby, E. and Martin, H. 2008. Mafic and felsic magma interactions in granites: the Hercynian Karkonosze pluton (Sudetes, Bohemian Massif). *Journal of Petrology*, **49**, 353–391.

Słaby, E., Seltmann, R., Kober, B., Műller, A., Galbarczyk-Gąsiorowska, L. and Jeffries, T. 2007b. LREE distribution patterns in zoned alkali feldspar megacrysts – implication for parental melt composition. *Mineralogical Magazine,* **71**, 193–217.

Słaby, E., Śmigielski, M., Śmigielski, T., Domonik, A., Simon, K. and Kronz, A. 2011. Chaotic three-dimensional distribution of Ba, Rb, Sr in feldspar megacrysts grown in an open magmatic system. *Contribution to Mineralogy and Petrology*, **162**, 889–1113.

Słaby, E., Martin, H., Hamada, M., Śmigielski, M., Domonik, A., Götze, J., Hoefs, J., Hałas, J., Simon, K., Devidal, J.-L., Moyen, J.-F. and Jayananda, M. 2012. Evidence in Archaean Alkali Feldspar Megacrysts for High-Temperature Interaction with Mantle Fluids. *Journal of Petrology*, **53**, 67–98.

Voronoi, G. 1907. Nouvelles applications des paramètres continus à la théorie des formes quadratiques. *Journal für die Reine und Angewandte Mathematik*, **133**, 97–178.

West, B.J. 1990. Fractal physiology and chaos in medicine. World Scientific; Singapore.

Yang Z.Y. and Lo S. C. 1997. An Index for Describing the Anisotropy of Joint Surfaces. *International Journal of Rock Mechanics and Mining Sciences*, **34**, 1031–1044.

Yoeli, P. 1965. Analytical hill shading. *Surveying and Mapping,* **25**, 573–579.

Zhou, Q. and Liu, X. 2004. Analysis of errors of derived slope and aspect related to DEM data properties. *Computers & Geosciences*, **30**, 369–378.

Manuscript submitted: 2nd August 2011
Revised version accepted: 15th January 2012